

# VALIDATION OF A THREE-DIMENSIONAL HEAD PHANTOM FOR IMAGING DATA

**Jolanta Podolszańska**

Częstochowa University of Technology, Częstochowa, Poland

**Abstract.** This paper presents the research results on the design of a three-dimensional head phantom for cone beam projection. The head model is based on a Shepp-Logan mathematical head model, which is used to simulate the operation of the CT scanner. The model is then compared with the reference data for structural similarity, reasoning, and shape. The geometric parameters of the obtained images are investigated. The reconstructed image is analyzed using the FDK method. The results show that the geometric parameters directly correlate with the number of projections. A mathematical framework of cone beam 3D reconstruction via the first derivative of the radon transform is presented.

**Keywords:** computed tomography, FDK reconstruction, 3D mathematical phantom, Shepp-Logan phantom

## WALIDACJA TRÓJWYMIAROWEGO FANTOMU GŁOWY DLA DANYCH OBRAZOWYCH

**Streszczenie.** W artykule przedstawiono wyniki badań nad projektem trójwymiarowego fantomu głowy do projekcji wiązki stożkowej. Model głowy jest oparty na matematycznym modelu głowy Shepp-Logan, który jest używany do symulacji działania skanera CT. Model jest następnie porównywany z danymi referencyjnymi pod kątem podobieństwa strukturalnego, rozumowania i kształtu. Badane są parametry geometryczne uzyskanych obrazów. Zrekonstruowany obraz jest analizowany przy użyciu metody FDK. Wyniki pokazują, że parametry geometryczne mają bezpośredni związek z liczbą projekcji. Przedstawiono matematyczne ramy rekonstrukcji 3D wiązki stożkowej za pomocą pierwszej pochodnej transformaty radonowej.

**Słowa kluczowe:** tomografia komputerowa, rekonstrukcja FDK, trójwymiarowy matematyczny model fantomu, fantom Shepp-Logan

## Introduction

Using phantoms as a standard for head imaging simulation and reconstruction has allowed for examination without interference by the human body, which is crucial to avoid potential damage caused by X-rays. Specifically, the Shepp-Logan phantom was used to reconstruct magnetic resonance imaging (MRI) and for k-space simulation. However, the CT version is the only one to include the radiation mitigation properties of the head and brain. The phantom version of the MRI was not adapted to MR physics, so comparisons and validations of the model are not conducted based on various studies. This work focuses exclusively on the CT-adapted phantom and aims to present the existing implementations of the Shepp-Logan model and its modifications for simulation purposes.

### 1. 3D Cone-Beam Geometry

In CT, spiral scanning uses a specific activation protocol. This involves rotating the gantry simultaneously as the bed moves with the patient. The hypothesis is that the object scanning will remain in place, but this happens only if the source follows the spiral trajectory. In 2D geometry, the source trajectory is represented by vectors.

$$x_{focal} = \begin{pmatrix} D_1 \sin \beta \\ -D_1 \cos \beta \\ z_{start\_pos} \end{pmatrix}$$

The spiral scanning standard can express the source trajectory by the formula.

$$z_{focal} = \left[ z_{start\_pos}; z_{stop\_pos} = z_{start} \frac{d \cdot \beta_{stop}}{2\pi} \right]$$

For the reconstruction of spiral scanning, interpolation methods are used. A gantry with a four-angular range is required for complete scanning reconstruction to create a complete fan beam sinogram. However, the X-ray fan beam passes through these two segments at the beginning and end of the spiral path with a length of  $d$  at each angle at least once.

The inversion of the three-dimensional Radon transform  $R^3$  is obtained using an equation.

$$f(x) = -\frac{1}{8\pi} R^3 \left[ \frac{\partial^2}{\partial r^2} r(r\alpha) \right]$$

The application of the Radon transformation equation in 3D has been studied by scientists for decades. Reconstruction of projection data obtained in cone-beam geometry is a priority, as it is the geometry used in volumetric tomography with 2D detectors. A correct reconstruction is only possible if all planes intersect the radiation source's path at least once, later called the Tuy-Smith data sufficiency condition [6]. Based on Tuy's formula, Grangeat proposed a complete solution: to use the radiation derivative of the three-dimensional Radon transformation as an extract from the linear integrals extracted from the geometry of the cone beam. However, this solution is associated with the problem of numerical instability [7].

It is worth mentioning that accurate 3D reconstruction has limited practical application in the real world. The most commonly used source trajectory for most CT scanners is circular motion, which does not satisfy the Tuy-Smith sufficiency condition. To cope with the incompleteness of the data, researchers have worked on various trajectories; among them, only the circle and the spiral with constant pitch and radius have found significant applications. Therefore, approximate rather than exact algorithms are the most widely used in practical cone beam reconstruction. The most commonly used method for approximate cone beam reconstruction was derived by Feldkamp, Davis, and Kress (Feldkamp 1984 [8]).

### 1.1. FDK Method

In 1984, Feldkamp, Davis, and Kress introduced an algorithm for cone beam circular tomography reconstruction called the approximation method. This method is named so because the reconstructed result will differ slightly from the actual object, no matter how high the measurement resolution is. Despite this, the algorithm is favored for its simplicity and is widely used for cone beam reconstruction. Unlike the other methods, the FDK algorithm is unique in handling truncated data in the longitudinal direction. Initially designed for planar detectors, the FDK algorithm requires pre-weighting factors that depend on fan and cone angles and splicing with a ramp filter.

$$\bar{p}^F(\beta, a, b) = \left( \frac{R}{\sqrt{R^2 + a^2 + b^2}} p^F(\beta, a, b) \right) * g^P(a)$$

The pre-weighted and filtered projections are back-projected to the reconstruction volume.

$$f_{FDK}(x, y, z) = \int_0^{2\pi} \frac{R^2}{U(x, y, \beta)} (\beta, a(x, y, \beta), b(x, y, z, \beta)) d\beta$$

where:

$$b(x, y, z, \beta) = z \frac{R}{R + x \cos \beta + y \sin \beta}$$

When dealing with discrete cases, the sum of projection angles replaces the integral. The points in spiral geometry share similarities with those in the fan beam, with a longitudinal coordinate added to account for the detector's axial extension. The Feldkamp algorithm operates under the premise that the acquisition geometry of a conical beam should not differ from that of a multiplanar fan beam. This algorithm suits a planar detector system, where projection data can be interpolated onto a Cartesian grid. In contrast, Schaller's 1998 paper suggests that the algorithm should not filter along straight lines but rather along curved curves on a cylindrical detector. This method's calculation is quite similar to the primary FDK method, starting with ramp filtering.

$$\bar{p}(\beta, \gamma, q) = \left( \cos \gamma \frac{R}{\sqrt{R^2 + q^2}} p(\beta, \gamma, q) \right) * g(a)$$

The FDK algorithm utilizes a filtered approach to solve reconstruction tasks using computation efficiently. Due to its effectiveness, it has been widely adopted in commercial medical scanners and remains a leading technique in modern CT.

### 2. Two-dimensional Shepp-Logan mathematical head model

The two-dimensional Shepp-Logan mathematical head model was developed in 1974 [1] to simulate head and brain image reconstruction in CT and projection reconstruction. To mimic the head's geometric and X-ray attenuation properties, the model used ten ellipses (table 1) of varying size (grey levels) and material density.

Table 1. A function describing a phantom as the sum of 10 ellipses inside a 2x2 square

No. ellipse	Distance from the center of the image	x-axis	y-axis	Theta	Greyscale
1	(0, 0)	0.69	0.92	0	2
2	(0, -0.0184)	0.66	0.87	0	-0.98
3	(0.22, 0)	0.11	0.31	-18°	-0.02
4	(-0.22, 0)	0.16	0.41	18°	-0.02
5	(0, 0.35)	0.21	0.25	0	0.01
6	(0, 0.1)	0.046	0.046	0	0.01
7	(0, -0.1)	0.046	0.046	0	0.01
8	(-0.08, -0.605)	0.0446	0.023	0	0.01
9	(0, 0.605)	0.023	0.023	0	0.01
10	(0.06, -0.605)	0.023	0.046	0	0.01

The original projection number was 180x160, while the current image resolution is 256x256 or 512x512.



Fig. 1. Sheep-Logan mathematical phantom with ten ellipses source: own implementation in Python language

### 3. Three-dimensional Sheep-Logan mathematical head model

In 1980, the Sheep-Logan phantom was updated with 17 ellipsoids to accommodate three-dimensional acquisition images and included new anatomical structures like ears, eyes, nose, and mouth. However, during the latter part of the 1980s, the 3D phantom was simplified to just ten ellipsoids by removing six anatomical regions and the blood clot region, previously named the subdural hematoma area. In 1994, the phantom was enhanced again by adding two tumor regions, bringing the total ellipsoids to 12.

3D head phantoms in imaging medicine research make it possible to simulate various clinical conditions, directly improving imaging techniques and treatment planning. For phantoms to be helpful in a clinical setting, they must be carefully validated for their similarity to accurate imaging data. Researching the effectiveness of reconstruction algorithms without testing them on the patient, directly exposing him to a high radiation dose, is challenging. Algorithms must undergo validation testing before being put into clinical use. Therefore, engineers responsible for reconstruction algorithms work mainly on computer simulations that mimic the operation of an accurate CT scanner [2].

Physical phantoms have been developed that fully provide a comprehensive evaluation of image acquisition. The phantom presented in three-dimensional space is an evolution of the two-dimensional phantom. It has an extension in the form of an additional dimension, represented by mathematical functions (table 2).

Table 2. 3D phantom description function, version with ten ellipses

No. ellipse	x-axis	y-axis	z-axis	a	b	c	α	Greyscale
1	0	0	0	6.9	9.20	9	0	2
2	0	0	0	0.62	8.74	8.8	0	0.98
3	-0.22	0	-0.25	0.41	0.16	0.21	-108	0.02
4	2.2	0	-2.5	3.10	1.10	2.2	-72	0.02
5	0	3.5	-2.5	2.10	2.50	5	0	0.01
6	0	1	-2.5	0.46	0.46	0.46	0	0.01
7	-0.8	-6.5	-2.5	0.46	0.23	0.20	0	0.01
8	0.6	-6.5	-2.5	0.46	0.23	0.20	90	0.01
9	0.6	-1.05	6.25	0.56	0.40	1	90	0.01
10	0	1	6.25	0.56	0.56	1	0	0.01

### 4. Methods

A set of different methods was used to validate the 3D head phantom. A three-dimensional model of the head phantom was created, then compared with reference data for structural similarity, reasoning, and shape. In addition, a qualitative and quantitative analysis of the phantom was performed by comparing the results obtained using accurate imaging data.

The physical CT scanner collects raw data during a patient's scan. To replicate this process, a three-dimensional Shepp-Logan model was utilized to generate data converted into raw data for a RAW extension. This extension is obtained when the scanner acquires data but has not yet undergone digital processing. A RAW image stores a broader range of dynamic and gray level scales than the final image format, containing most of the original image's information. The simulation involves two essential components: the CT scanner and the console used by the electrobiology technicians. A simulation has been developed to meet these requirements.

## 5. Results

Researchers utilized a Python-designed simulation environment to conduct a study. They employed a spiral beam reconstruction algorithm and processed data from a virtual head phantom into raw data. This data was then utilized to reconstruct the object further. The simulation aims to replicate the function of a CT scanner, extracting the necessary parameters for image reconstruction.

### 5.1. Raw data

During a scan, the X-ray beam gathers raw data, including all measured detector signals. These signals are then calibrated to account for fluctuations in lamp power and beam hardening. The attenuation properties of each X-ray signal and its correlation with beam position are also considered. Mathematical procedures like filtered back projection are used to reconstruct the CT images from the raw data. Furthermore, a different filter can reconstruct additional planes and images later. The computer uses the raw data to map local attenuation within the studied section [4].

In the axial (transverse) plane, every image comprises a grid of data points assigned a number indicating the X-ray attenuation at a specific point on the human body. This number is essentially a scaled version of the X-ray attenuation of water, referred to as a Hounsfield unit. The air is also accounted for through normalization. A CT number of -1,000 HU is assigned, and water is posted as 0 HU.

Modern CT scanners typically have a matrix size of  $512 \times 512$  pixels. The size of each pixel is determined by the reconstructed field of view and the matrix size. In body applications, the pixel size is usually between 0.6–0.8 mm, while for the brain, it is approximately 0.5 mm. The pixel size varies for bone imaging, ranging from 0.3–0.5 mm.

### 5.2. CT and console simulation in CT

The simulation software is designed to incorporate Feldkamp-type reconstruction from precomputed projection data. It's important to note that the spiral geometry parameters are fixed and cannot be altered during reconstruction. The geometry must remain consistent with the one used for generating the pre-calculated projection data set, which will be loaded through a specific method. To better understand the parameters used during the reconstruction, refer to the image in (figure 2).

```

detector_type: DetectorType.CT
mode: Mode.CONEBEAM
pixels_per_slice_nb: 64
detector_slice_nb: 64
slice_pitch_mm: 4
detector_shape: DetectorShape.PLANAR
sdd_mm: 750
sad_mm: 500
fan_angle_deg: 30
gantry_angles_nb: 360
angular_range_deg: 360
image_matrix_size_mm: [256 256 256]
voxel_size_mm: [2 2 2]
number of projections: 1474560

```

Fig. 2. Simulation parameters in simulation software

For the simulation, each axis of the voxel size measures 2 mm. A coarse reconstruction grid will be utilized to obtain the projection in a reasonable time. The reconstruction begins with a sinogram, a 3D array of line integrals. The shape of the collection is based on the 2D reconstruction, meaning the first two dimensions are used in the 2D sinograms. When using cone beam geometry, the projection data is referred to as radiographs of a 3D object. Expanding the sinogram with an additional dimension is all that's necessary to update it. Volumetric or spatial reconstruction is another term for 3D reconstruction.

### 5.3. Head model visualization

To properly simulate on the console, we must input the data for the reference object (phantom) and the pre-calculated projection data. Specifically, we are working with a 3D phantom of the Shepp-Logan head, which has been sampled on a  $256^3$  grid. It is crucial to transpose the data in the correct order to ensure accurate results in the subsequent steps.

For this solution, a Ram-Lak filter was utilized by generating a 3D array that included all the necessary copies of the 1D Ram-Lak filter. This array was then used to filter the projection data in the frequency domain. Like the western beam, weighting factors were computed for the projection data just before implementing the Ram-Lak filter. To accomplish this, a grid of detector coordinate values was established. These weighting factors will be used on the original projection data.

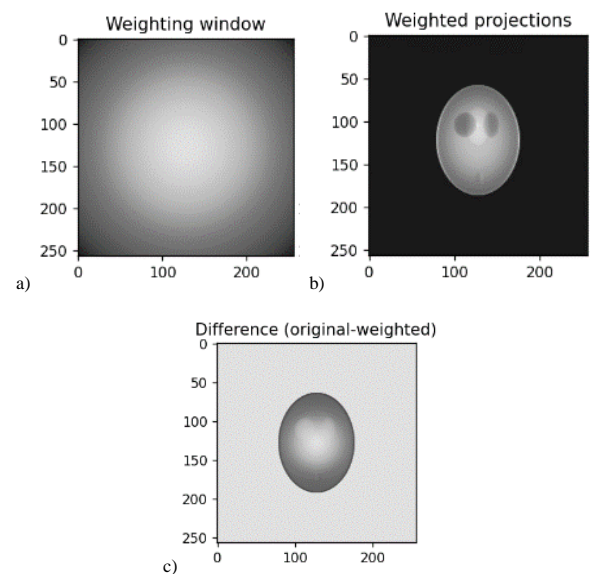


Fig. 3. Filtering: a) weighting window, b) weighted projections, c) difference between original and weighted image

In the next step, ramp filtering of the projections was performed. It is important to remember to properly arrange the input and output arrays so that the projection data is filtered line by line along the radial direction.

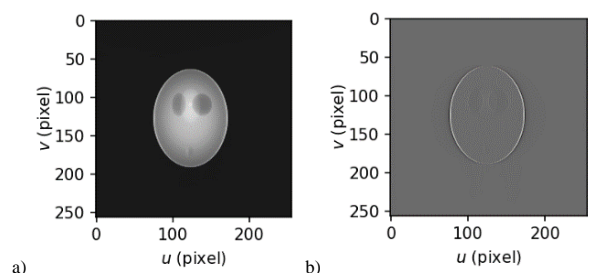


Fig. 4. Filtering: a) original model 3D Shepp-Logan, b) ramp filter applied to the model

A back projection of the cone beam was made. In this way, it will be possible to make a single view of the filtered radiographs. We will first select a single picture from the (filtered) projection data and create the auxiliary variables needed to calculate the  $w_{BP}$  weighting factor. We will perform a two-dimensional interpolation associated with the back projection on the cone beam.

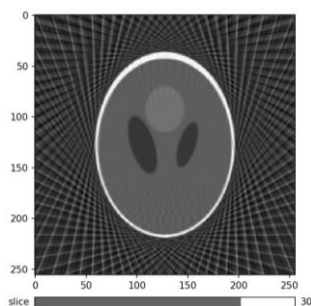


Fig. 5. Reconstruction with a limited number of projections

After a full back projection, we choose a volume with fewer cross-sections so that the reconstruction time does not burden the average computer. The number of cross-sections can be modified if we have a computer with more computing power. Of course, with the change in the number of cross-sections, the coordinate grids and weighting factors should be recalculated to cope with the new volume size.

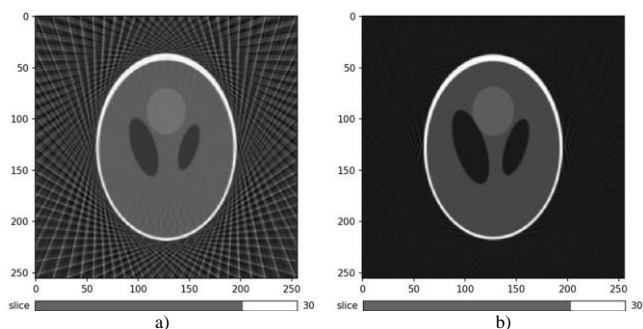


Fig. 6. Effect of reconstruction: a) without filtering, b) with filtering

The image volume was displayed using the matplotlib package (Fig. 4). The artifacts are due to solid angular subsampling. Partial volumes were reconstructed. The actual image reconstruction may take 5 to 10 minutes. The effect of the model reconstruction is shown below (Fig. 6).

## 6. Conclusions

This paper presents the research results on the design of a three-dimensional phantom for cone beam projection. The research included creating a simulation environment for a three-dimensional Shepp-Logan and reconstructing

the projection image using the FDK method. The paper presents a mathematical description of the head model and suggestions for the designed simulation. The experimental relationship between the geometric parameters of the obtained images was established. Various simulation parameters were investigated for the reconstructed image, including a photo with limited projections and a more significant number of forecasts. The simulation environment will be expanded in the future.

## Conflict of interests

The author declares no conflicts of interest.

## References

- [1] Batur A. et al.: Hounsfield unit density in the characterization of bile duct lesions. *Polish Journal of Radiology* 84, 2019, 397–401.
- [2] Dzierżak R., et al.: The influence of the normalization of spinal CT images on the significance of textural features in identifying defects in the spongy tissue structure. *Innovations in Biomedical Engineering*. Springer International Publishing, 2019.
- [3] Hansen P. C. et al.: *Computed tomography: algorithms, insight, and just enough theory*. Society for Industrial and Applied Mathematics, 2021.
- [4] Ilmavirta J., Monkkonen K.: X-ray tomography of one-forms with partial data. *SIAM Journal on Mathematical Analysis* 53(3), 2021, 3002–3015.
- [5] Panetta D., Camarlinghi N.: *3D Image Reconstruction for CT and PET: A Practical Guide with Python*. CRC Press 2020, 65–73.
- [6] Senchukova A.: *Learned image reconstruction in X-ray computed tomography*, 2020.
- [7] Sun W. et al.: Review of high energy x-ray computed tomography for non-destructive dimensional metrology of large metallic advanced manufactured components. *Reports on Progress in Physics* 85(1), 2022, 016102.
- [8] Tadeusiewicz R.: Komputerowe systemy wizyjne w zastosowaniach przemysłowych. *Utrzymanie Ruchu* 3, 2019, 14–21.
- [9] Withers P. J. et al.: X-ray computed tomography. *Nature Reviews Methods Primers* 1(1), 2021, 18.
- [10] Xu X. et al.: Review of electromagnetic vibration in electrical machines. *Energies* 11(7), 2018, 1779.
- [11] Zuo C. et al.: Transport of intensity equation: a tutorial. *Optics and Lasers in Engineering* 135, 2020, 106187.

**M.Sc. Eng. Jolanta Podolszańska**  
e-mail: jolanta.podolszanska@pcz.pl

In 2019 she started her doctoral studies at the Doctoral School of the Częstochowa University of Technology in the field of technical informatics and telecommunications. She is a research and teaching assistant at the UJD Mathematics and Computer Science Department.

Research interests: health informatics, artificial intelligence, programming in Python.

<http://orcid.org/0000-0002-6032-5654>

